

Synthesis and hydrodesulfurization (HDS) and hydrogenation (HYD) activity of dimolybdenum nitride

Yaojun Zhang, Zhaobin Wei, Weihong Yan, Pinliang Ying, Chunxin Ji, Xinsheng Li, Zhenhua Zhou, Xiuping Sun, Qin Xin *

State Key Laboratory of Catalysis, Dalian Institute of Chemical Physics, Chinese Academy of Sciences, Dalian 116023, PR China

Abstract

Various kinds of surface area γ -Mo₂N were synthesized by a topotactic reaction between MoO₃ and NH₃ under relatively mild conditions. It was found that the space velocity of NH₃ and the particle size of MoO₃ were very important for the synthesis of high surface area γ -Mo₂N in a large batch. The percent of micropore volume in the range of 20–30 Å gradually increased with increase of surface area. XRD results indicated that the intensities of diffraction peaks of high surface area γ -Mo₂N was different from those of low surface area. The measurements of catalytic activities for thiophene hydrodesulfurization and cyclohexene hydrogenation showed that high surface area γ -Mo₂N exhibited much higher activity than those of medium and low surface area γ -Mo₂N. Meanwhile, a hydrodesulfurizing mechanism of thiophene is proposed.

Keywords: Synthesis; Hydrodesulfurization (HDS) activity; Hydrogenation (HYD) activity; Dimolybdenum nitride

1. Introduction

Dimolybdenum nitride of high surface area is a particularly promising catalyst for heterogeneous catalytic reactions. In early studies γ -Mo₂N was used as a catalyst for ammonia synthesis [1], ethylene hydrogenation [2], ethane hydrogenolysis [3], hydrodenitrogenation [4] and hydrodesulfurization [5]. However, little attention has been paid to the catalytic properties of dimolybdenum nitride for competitive reactions of hydrodesulfurization (HDS) and hydrogenation (HYD). The primary purpose of this paper is to understand the details of Mo nitrides towards activity for thiophene HDS and cyclohexene HYD. To use the nitride efficiently in catal-

ysis, a powder of it must be prepared with a high specific area. However, known synthesis methods for γ -Mo₂N were quite complicated in previous investigations [5,6]. So, another purpose of this paper was to carry out a relatively gentle synthesis method as compared with the methods mentioned above.

2. Experimental

2.1. Catalyst synthesis

A series of samples were synthesized in a reactor (0.6 m long, 8 mm i.d. quartz tube) by a temperature-programmed reaction of 3 g MoO₃ under flowing NH₃. The starting material MoO₃ was pressed into pellets and sieved to yield

* Corresponding author.

approximately 20–100 mesh particles. The temperature programmed reaction was divided into three segments. First, a heating rate of 5 K/min from room temperature to 573 K was used. Second, heating rates from 1 K/min to 10 K/min was employed in different reactions in the temperature range 573 to 973 K and finally the sample was held for 2 h at 973 K. After that, the furnace was opened and the sample was rapidly cooled to room temperature in flowing NH_3 . The sample was then passivated in mixtures of N_2 and a small amount of O_2 for 12 h to form a stable material.

2.2. Characterization

2.2.1. Surface area and pore size distribution

BET surface area and pore size distribution of samples were determined at liquid nitrogen temperature by a Micromeritics ASPA-2000 adsorption analyzer.

2.2.2. X-ray diffraction

The bulk structure of the passivated sample was characterized by a Regaku Rotaflex (Ru-200B) powder X-ray diffractometer ($\text{Cu K}\alpha$ radiation) and a computer system was used for data collection.

2.3. Evaluation of catalytic activities

All reactions were carried out in a middle pressure stainless-steel fixed-bed microreactor with 0.5 g passivated catalyst supported between pads of quartz sand. The reaction temperature was 573 K and the hydrogen pressure was 3 MPa. The liquid feeds, consisting of 24 wt% cyclohexene, 1 wt% thiophene dissolved in 75 wt% cyclohexane was delivered using a syringe pump. The liquid hourly space velocity (LHSV) was 18 h^{-1} and the hydrogen to liquid volume ratio was 700. Before reaction each catalyst was first pre-reduced at 673 K in 3 MPa hydrogen for 1 h and then cooled to 573 K. The effluents were analyzed by gas chromatography with a flame ionization detector (filled column, Car-

bowax, Shanghai, model 103). Data processing was completed by a computer system.

3. Results and discussion

3.1. Synthesis of high surface area $\gamma\text{-Mo}_2\text{N}$

In order to improve the synthetic conditions of high surface area $\gamma\text{-Mo}_2\text{N}$, the particle size of the precursor, space velocity of NH_3 , heating rate and passivation procedure were carefully examined. Experiments showed that the particle size has a serious effect on NH_3 diffusion into and out of the synthesis bed. It was found that a particle size of 20–40 mesh was desirable for the production of high surface area $\gamma\text{-Mo}_2\text{N}$ (Table 1, $\text{Mo}_2\text{N-1}$ to $\text{Mo}_2\text{N-3}$). The NH_3 space velocity was the most important factor as previously reported [7]. When the space velocity of NH_3 was decreased from $40\,000 \text{ h}^{-1}$ to 4000 h^{-1} , the surface area declined approximately 11 times from $140 \text{ m}^2/\text{g}$ to $13 \text{ m}^2/\text{g}$ (Table 1, $\text{Mo}_2\text{N-4}$ and $\text{Mo}_2\text{N-6}$). The surface area also decreased rapidly with increased heating rate from a heating rate of 1 K/min ($\gamma\text{-Mo}_2\text{N-1}$, $S_{\text{BET}} = 87 \text{ m}^2/\text{g}$) which was raised to 3 K/min ($\gamma\text{-Mo}_2\text{N-7}$, $S_{\text{BET}} = 13 \text{ m}^2/\text{g}$) the surface area lost $78 \text{ m}^2/\text{g}$ under the same space velocity of NH_3 . The reason that both a smaller space velocity and a faster heating rate lead to a lower

Table 1
Effect of synthesis condition on $\gamma\text{-Mo}_2\text{N}$ surface area^a

Catalyst code	MoO_3 particle (mesh)	Space velocity of NH_3 (h^{-1})	Heating rate (K/min)	Surface area (m^2/g)
MoO_3				1
$\text{Mo}_2\text{N-1}$	20–40	8000	1	87
$\text{Mo}_2\text{N-2}$	40–60	8000	1	82
$\text{Mo}_2\text{N-3}$	80–100	8000	1	74
$\text{Mo}_2\text{N-4}$	20–40	40000	1	140
$\text{Mo}_2\text{N-5}$	20–40	30000	1	123
$\text{Mo}_2\text{N-6}$	20–40	4000	1	13
$\text{Mo}_2\text{N-7}$	20–40	8000	3	19
$\text{Mo}_2\text{N-8}$	20–40	8000	5	17
$\text{Mo}_2\text{N-9}$	20–40	8000	10	15

^a Note: the amount of MoO_3 in each batch was 3 g.

surface area γ -Mo₂N is that the produced water was difficult to remove from the reactor bed during oxido-reduction ($2\text{MoO}_3 + 4\text{NH}_3 = \text{Mo}_2\text{N} + 6\text{H}_2\text{O} + 3/2\text{N}_2$). It could cause hydrothermal sintering and induced aggregation of the resultant microparticles.

In previous methods [5,6] synthetic conditions of high surface area Mo nitride (usually $S_{\text{BET}} > 100 \text{ m}^2/\text{g}$) were quite difficult and the amount of the starting material MoO₃ in each batch was much less than 1 g. However, some synthetic conditions were greatly improved in our experiments. The heating rate of the reaction segment was increased from the original 0.6 K/min to 1 K/min, the space velocity of NH₃ was only one-tenth of the reported methods, and the amount of precursor approached 3 g.

3.2. Pore size distribution of γ -Mo₂N

The pore size distribution of low ($S_{\text{BET}} < 20 \text{ m}^2/\text{g}$), medium ($20 \text{ m}^2/\text{g} < S_{\text{BET}} < 100 \text{ m}^2/\text{g}$) and high surface area ($S_{\text{BET}} > 100 \text{ m}^2/\text{g}$) γ -Mo₂N are shown in Fig. 1. The pore size distribution of low surface area γ -Mo₂N is in the range 20–500 Å. Nevertheless, the pores size of medium and high surface area γ -Mo₂N was predominately concentrated in the diameter range of 20–50 Å. At the same time, the percentage of micropore volume in the range 20–30 Å gradually increased with increase of γ -Mo₂N surface area (in Table 2).

3.3. XRD results

The bulk structure of passivated samples was characterized by XRD. The peaks of γ -Mo₂N

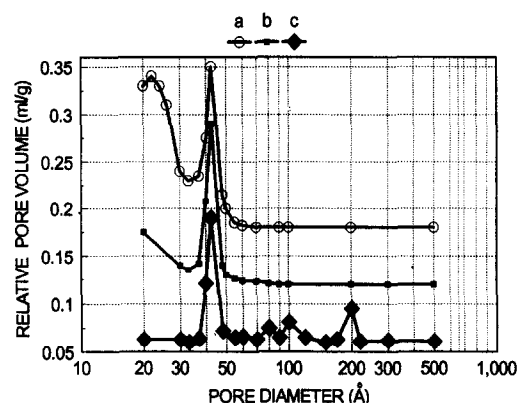


Fig. 1. Desorption pore diameter distribution of γ -Mo₂N: (a) Mo₂N-4, (b) Mo₂N-2 and (c) Mo₂N-6.

were located at 37.1, 43.1, 75.2, 62.7 and 79.1, respectively. The locations and intensities of diffraction peaks for low surface area γ -Mo₂N were in agreement with the literature [8]. But the (200) plane ($2\theta = 43.1$) of the high surface area γ -Mo₂N was more intense than that of the low surface area γ -Mo₂N. The intensities ratio of (200)/(111) was greater than 2.7 for the highest surface area γ -Mo₂N (Mo₂N-4). This type of texture may be a result of topotactic reaction of MoO₃ with NH₃ transferred into pseudomorphic Mo nitride.

In order to find a reasonable method for the synthesis of γ -Mo₂N, the nitriding mechanism of MoO₃ in the temperature range from 573 to 973 K was studied by XRD. The precursor MoO₃ showed no phase change until a reaction temperature of 673 K was reached. XRD results indicated that one phase was MoO₂ and the other was an unknown material which was ascribed to an oxynitride (Mo₂O_xN_{1-x}) according to previous investigations [5,7]. At a tempera-

Table 2
Pore size distributions

Catalyst code	S_{BET} (m ² /g)	Pore volume (ml/g)	Average pore size (Å)	Pore volume (%)		
				20–30 (Å)	30–50 (Å)	50–500 (Å)
Mo ₂ N-4	140	0.086	24.8	56	36	8
Mo ₂ N-2	82	0.070	32.2	29	60	11
Mo ₂ N-6	13	0.022	68.9	11	10	74

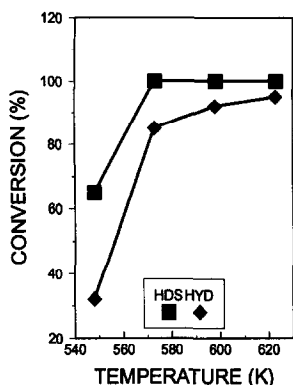


Fig. 2. Conversion of thiophene and cyclohexene over $\text{Mo}_2\text{N-4}$ versus temperature, LHSV = 18 h^{-1} , $\text{H}_2 = 3 \text{ MPa}$.

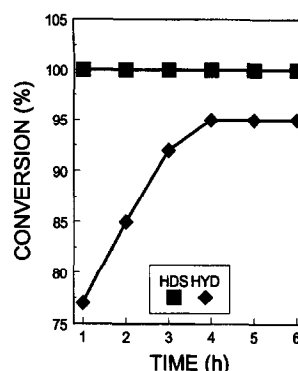


Fig. 3. Conversion of thiophene and cyclohexene over $\text{Mo}_2\text{N-4}$ versus time at 573 K, LHSV = 18 h^{-1} , $\text{H}_2 = 3 \text{ MPa}$.

ture of 973 K and successfully holding for 2 h at 973 K, XRD results showed that the phases of MoO_3 and the unknown material completely disappeared and only the $\gamma\text{-Mo}_2\text{N}$ phase was left. However, Because the transformation of MoO_3 into $\gamma\text{-Mo}_2\text{N}$ is a topotactic reaction, $\gamma\text{-Mo}_2\text{N}$ has a well-defined crystallographic orientation relative to the parent MoO_3 . In particular, the (100) planes of $\gamma\text{-Mo}_2\text{N}$ are parallel to the (010) planes of MoO_3 [5,6]. It may be of great advantage to produce high surface $\gamma\text{-Mo}_2\text{N}$ with a slow heating rate in the temperature range from 573 to 973 K.

3.4. Catalytic activities

The thiophene hydrodesulfurization (HDS) and cyclohexene hydrogenation (HYD) activities of each catalyst were tested. The dependence of conversion of HDS and HYD on temperature over passivated Mo_2N are given in Fig. 2. The conversion of thiophene was 65% at 548 K and then rapidly reached 100% at 573 K. The conversion of cyclohexene HYD gradually increased with increasing temperature. Fig. 3 shows conversions of HDS and HYD versus time over $\text{Mo}_2\text{N-4}$ catalyst. The conversion of thiophene HDS was 100% and cyclohexene HYD finally approached 95% during catalytic reactions of 6 h.

High, medium and low surface area catalysts

were examined for thiophene HDS and cyclohexene HYD activities as shown in Fig. 4. Thiophene conversion was found to be proportional to the surface area of the catalyst. Meanwhile, the conversion of thiophene HDS was always larger than cyclohexene HYD except for the catalyst of low surface area. $\gamma\text{-Mo}_2\text{N}$ with a surface area up to $140 \text{ m}^2/\text{g}$ for HDS HYD exhibited a similar magnitude compared with a commercial sulfide $\text{Co-Mo}/\text{Al}_2\text{O}_3$ catalyst. After a 6 h run, the catalyst of high and medium surface area $\gamma\text{-Mo}_2\text{N}$ burnt brightly when it was exposed to air, which indicated that the high and medium surface area catalysts showed higher activities than the low surface area catalyst.

We suggest that high activities are mainly

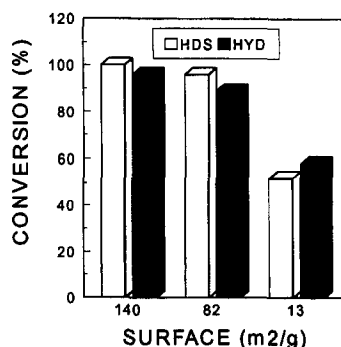
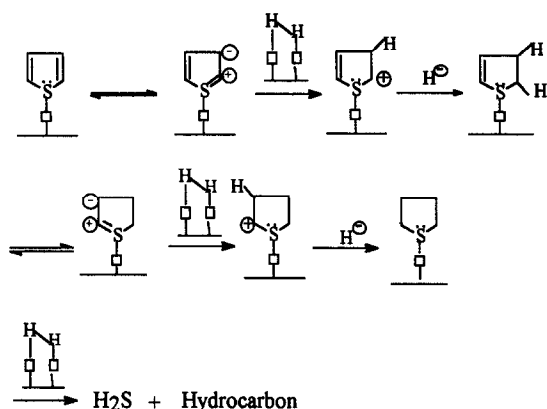


Fig. 4. Effects of surface area on the conversion of thiophene HDS and cyclohexene HYD at 573 K, LHSV = 18 h^{-1} , $\text{H}_2 = 3 \text{ MPa}$.



Scheme 1.

related to chemisorption of hydrogen on the surface of γ - Mo_2N . Haddix et al. found that hydrogen dissociatively adsorbs on the high surface area γ - Mo_2N [9] and hydrogen adsorption on γ - Mo_2N showed a different behaviour from hydrogen adsorption on MoS_2 [10]. Choi et al. considered that the hydrogen could migrate into the subsurface during exposure to H_2 at elevated temperatures [11]. While thiophene and cyclohexene contacted with the surface of the catalyst, both of them could be attacked by chemisorbed H_2 . The conversion of thiophene was higher than that of cyclohexene for high and medium surface area γ - Mo_2N . We suggest that the oxygen was removed from the surface layer of γ - Mo_2N during catalyst pre-reduction. The increase of nitrogen deficient sites led to strong Lewis acid sites of molybdenum. The strong Lewis basic sites of sulfur in the thiophene heterocyclic ring compared with cyclohexene was easily attacked by a Lewis acid. In addition, the five member heterocyclic rings are much more electron-rich than cycloalkene. So it is more liable to attack by electrophiles. The electrophilic addition mechanism is shown in Scheme 1.

4. Conclusions

For the preparation of high surface area γ - Mo_2N , mild conditions were developed by a temperature programmed reaction of NH_3 and MoO_3 . The volume percent in the micropore range 20–30 Å increased with increase of surface area. The XRD results indicated that the intensities of the diffraction peaks of high surface area γ - Mo_2N are different from that of low surface area γ - Mo_2N . The catalyst of high surface area γ - Mo_2N exhibited a high catalytic activity for thiophene HDS and cyclohexene HYD.

Acknowledgements

We thank engineers Yanfen Miao and Li Wang who have been working in the State Key Laboratory of Catalysis for their contribution to our surface area, pore size distribution and X-ray diffraction measurements.

References

- [1] L. Volpe and M. Boudart, *J. Phys. Chem.*, 90 (1986) 4878.
- [2] Y. Shigehara, *Nippon Kagaku Kaishi*, 4 (1977) 470.
- [3] G.S. Ranhotra, A.T. Bell and J.A. Reimer, *J. Catal.*, 108 (1987) 40.
- [4] J.C. Schlatter, S.T. Oyama and J.E. Metcalf, *Ind. Eng. Chem. Res.*, 27 (1988) 1648.
- [5] E.J. Markel and J.W. Van Zee, *J. Catal.*, 126 (1990) 643.
- [6] R.S. Wise and E.J. Markel, *J. Catal.*, 145 (1994) 335.
- [7] J.G. Choi, R.L. Curl and L.T. Thompson, *J. Catal.*, 146 (1994) 218.
- [8] W.F. McClune, *JCPDS International Centre for Diffraction Data*, 1989.
- [9] G.W. Haddix, J.A. Reimer and A.T. Bell, *J. Catal.*, 108 (1987) 50.
- [10] J. Polz, H. Zeilinger, B. Muller and H. Knozinger, *J. Catal.*, 120 (1989) 22.
- [11] J.G. Choi, J.R. Brenner and C.W. Colling, *Catal. Today*, 15 (1992) 201.